Cooling and societal change during the Late Antique Little Ice Age from 536 to around 660 AD

Ulf Büntgen[1,2,3*], Vladimir S. Myglan[4], Fredrik Charpentier Ljungqvist[5,6], Michael McCormick[7], Nicola Di Cosmo[8], Michael Sigl[9], Johann Jungclaus[10], Sebastian Wagner[11], Paul J. Krusic[12], Jan Esper[13], Jed O. Kaplan[14], Michiel A.C. de Vaan[15], Jürg Luterbacher[16], Lukas Wacker[17], Willy Tegel[18] and Alexander V. Kirdyanov[4,19]

[1]Swiss Federal Research Institute WSL, Birmensdorf, Switzerland. [2]Oeschger Centre for Climate Change Research, Bern, Switzerland. [3]Global Change Research Centre AS CR, Brno, Czech Republic. [4]Siberian Federal University, Krasnoyarsk, Russia. [5]Department of History, Stockholm University, Sweden. [6]Bolin Centre for Climate Research, Stockholm University, Sweden. [7]Initiative for the Science of the Human Past (SoHP), Harvard University, Cambridge, USA. [8]Institute for Advanced Study, School of Historical Studies, Princeton, USA. [9]Paul Scherrer Institute PSI, Villigen, Switzerland. [10]Max Planck Institute for Meteorology, Hamburg, Germany. [11]Institute for Coastal Research, Helmholtz-Zentrum Geesthacht, Geesthacht, Germany. [12]Navarino Environmental Observatory, Messinia, Greece. [13]Department of Geography, Johannes Gutenberg University, Mainz, Germany. [14]University of Lausanne, Institute of Earth Surface Dynamics, Lausanne, Switzerland. [15]Department of Linguistics and Information Sciences, University of Lausanne, Switzerland. [16]Department of Geography, Justus Liebig University, Giessen, Germany. [17]Laboratory for Ion Beam Physics, ETHZ, Zurich, Switzerland. [18]Chair of Forest Growth, Albert-Ludwigs University, Freiburg, Germany. [19]VN Sukachev Institute of Forest SB RAS, Krasnoyarsk, Russia. *email: buentgen@wsl.ch

The supposed role of climate change on societal reorganizations in Europe[1,2] and Asia[3,4] during the first half Common Era (CE) is difficult to prove without adequate annually resolved and absolutely dated climate proxy archives[5,6]. Interpretation of concurrences between cooling in the 6th century and pandemic[7,8], rising and falling civilizations[1-6], human migrations and political turmoil[8-13] lacks understanding of scalar and causal mechanisms. Here we use tree-ring chronologies from the Russian Altai and Austrian Alps to reconstruct summer temperatures over the past two millennia. In both regions, conditions during Roman and recent times were warmer than throughout the medieval period. Unprecedented, long-lasting and spatially synchronized cooling following a cluster of large volcanic eruptions in 536, 540 and 547 CE[14], was likely sustained by ocean and sea-ice feedbacks[15,16], superimposed on a solar minimum[17]. This newly defined Late Antique Little Ice Age (LALIA, 536 to ~660 CE) exceeded the LIA in severity. Covering much of the Northern Hemisphere, it should be considered as an additional environmental factor contributing to the establishment of the Justinian plague[7,8], transformation of the eastern Roman and collapse of the Sasanian Empire[1,2,5], movements out of the Asian steppe and Arabian Peninsula[8,11,12], spread of Slavic-speaking people[9,10], and upheavals in China[13].

Annually resolved and absolutely dated insight into late Holocene climate variability is crucial in order to distinguish anthropogenic from natural forced variation[18], and to evaluate the performance of climate model simulations[19]. Spatially well-distributed palaeoclimatic archives are also essential for answering questions surrounding possible relationships between climate variability and human history[5,6]. However, around the world today, there are only 13 temperature sensitive tree-ring chronologies that span the entire CE (Table S1).

Absence of precise climate reconstructions for large parts of central Asia has impeded accurate assessment of environmental factors that may have driven momentous interaction between steppe pastoralists and peripheral sedentary civilizations. At the same time, summer warmth between June and August (JJA) is known to control tree-ring formation at higher altitudes in the Altai Mountains[20], where continental climate supports the preservation of dead wood on the ground. Despite a long history of habitation by pastoral nomads[21], >60% of this region is still forested, with Siberian larch (*Larix sibirica* Ldb.) being the dominant species. Though widespread steppe environments constitute an enzootic wildlife reservoir for the plague bacterium *Yersinia pestis*[22], it remains unclear if historical pandemics in Europe originated from natural infection foci in Asia[23], and what role climate might have played in their epidemic onset. Moreover, root causes for human migrations out of the central Asian steppes between the 4th and 7th centuries CE have not been unambiguously identified[3,4].

Here, we present tree-ring width (TRW) samples from 152 living and 508 relict larch specimens collected at five high-elevation sites in the Russian Altai-Sayan Mountains (Fig. S1; Table S2). All 660 TRW series share a significant fraction of common growth variability (Fig. S2a), with their start and end dates distributed between 359 BCE and 2011 CE (Fig. S2b). This dataset has a minimum replication of ten series in 98 CE and a maximum of 240 series in 1279 CE. The mean tree age is 355 years and the average annual growth rate is 0.44 mm (Table S2). Reduced tree recruitment between ~350 and 650 CE implies cooler summers (Fig. S2c), whereas intensified germination during medieval times, and again ~1500 CE suggests the opposite. Abundant dead wood at all sampling sites refutes disturbance from nomadic settlements and grazing by domestic animals. The cosmogenic ^{14}C radiocarbon time marker of 775 CE[24] provides independent isotopic age confirmation of the dendrochronological dates (Fig. S3; Supplementary Information). A wavelet power spectrum of the high-frequency Altai TRW chronology displays no sign of pulse-like disruptions (Fig.

S4), such as those caused by cyclic outbreaks of the larch budmoth (*Zeiraphera diniana* Gn.) in the European Alps[25].

Though separated by ~7600 km, the new Altai TRW chronology (Supplementary Information) shares remarkably high agreement with dendroclimatological findings from the Austrian Alps[5] (the Alpine chronology; Fig. 1a). Statistically significant (p <0.001) correlations between the Asian and Alpine records infer a large-scale teleconnection pattern associated with the upper troposphere (200 hPa) geopotential height and meridional velocity fields; the circumglobal wave train[26]. Coupled climate model simulations back to 850 CE[27] also reproduce co-varying climate patterns in Europe and central Asia (Fig. S5), furthermore suggesting that warm summers with anomalous high-pressure conditions most likely coincide with below-average precipitation totals across these regions (Fig. S6).

Both TRW chronologies from the Alps and the Altai capture a substantial fraction of instrumental-based, 20th century regional JJA temperature variability (Fig. S7). Significant proxy-target agreement at all frequency domains refutes any 'divergence issue' in both chronologies (Supplementary Information). Although the spatial temperature signature of the Alpine record is larger than the one from the Altai (Fig. 1b), both are nearly geographically identical to the correlation fields produced by observational JJA temperatures over the same region (Fig. 1b inset; Fig. S8). The warmest reconstructed summer in central Asia was 982 CE (+1.6°C $_{\text{with respect to 1961-1990}}$), and six of the 12 warmest summers have occurred since 2004 (Fig. 2a). The summer of 2010, associated with an exceptional heatwave over western Russia[28], is only the 12th warmest. The Alpine record's warmest summer (+3.5°C $_{\text{wrt. 1961-1990}}$) coincided with the European heatwave of 2003[5] (Fig. 2b). Despite slightly different uncertainty ranges (Fig. S9), the warmest decade in both reconstructions is the most recent. The coldest central Asian and European summers are 172 and 1821 CE, respectively (-4.6 and -3.3°C $_{\text{wrt. 1961-1990}}$). The 540s were the coldest and second coldest decade in the Altai and Alpine reconstruction, respectively (-3.2 and -1.9°C $_{\text{wrt. 1961-1990}}$). Of the 20 coldest central

Asian (European) summers, 13 (5) occurred in the 6th century after 536 CE. Thirteen (5) out of the 20 coldest decades in the Altai (Alpine) record fall in the 6th and 7th centuries.

Newly dated bipolar ice cores describe a large volcanic eruption at northern high-latitudes in March 536 CE[14], which injected huge amounts of aerosol into the stratosphere (an estimated global forcing of -11.3 W m^{-2}). Another (tropical) eruption in 540 (-19.1 W m^{-2}) even exceeded the forcing of Tambora in April 1815 (-17.2 W m^{-2}), and was followed by a smaller but still substantial eruption in 547 (-1.1 W m^{-2}) (Fig. 2c). The abrupt summer cooling after this unique sequence of eruptions was probably sustained by positive feedback loops of ocean-heat content and sea-ice extension[15,16] (Supplementary Information), with additional forcing likely contributed by the exceptional 7th century solar minimum[17] (Fig. 2d). As a result, the striking cold phase from 536 to ~660 CE is hereafter termed Late Antique Little Ice Age (LALIA). Independent evidence for this episode, which conceivably exceeded the severity of all LIA type events (Fig. 2), is found in a wide range of diverse proxy archives from the Northern Hemisphere (Fig. 3; Table S3). Due to changes in the Earth axis (a stronger inclination angle), extra-tropical summer shortwave insolation was higher than present-day[29], making the LALIA cooling even more outstanding.

Superposed epoch analyses (SEA) centered on the 20 largest volcanic forcings of the CE (Table S4) detects distinct post-eruption depressions in both the Alpine and Altai reconstructions (Fig. S10). Sharp and immediate summer cooling was stronger under the continental climate of central Asia in comparison to Europe where ocean-induced thermal inertia may have a mitigating effect. Patterns of volcanic-driven summer cooling also differ in space and time (Fig. S11). Though the thermal shock after the cluster of eruptions in 536, 540 and 547 CE is evident in both reconstructions, the early-19th century cooling after the unnamed eruption in 1809 and Tambora in 1815 is less prominent in the Altai. Cross-spectral analysis indicates maximum coherency between the Alpine and Altai records on longer time-

scales (Fig. S12), which might be explained by a Eurasian-wide wave train-like teleconnection[26,27] (Figs. S5-S6).

Coherent low-frequency behaviour in the Altai and Alpine records is further reflected by centennial-scale Eurasian temperature variability (Fig. S13a; Table S5): The generally warmer conditions prevailing in the first centuries CE until ~300 CE, from ~800-1200 CE, and again in the 20th century, were interrupted by the LALIA and several LIA type events between ~1300 and 1850 CE. Independent hydroclimatic proxies from Europe and Asia describe dry conditions in the 12th century, and from ~1400-1700 CE (Fig. S13b). While a long-term, pre-industrial negative temperature trend reflects the role of orbital forcing[29] (Fig. S14a), this drift is less conspicuous in hydroclimate (Fig. S14b).

Though associated with uncertainty, the LALIA – during which the fraction of pastoral and agricultural land use in central Europe and the Mediterranean appears exceptionally low (Fig. S15) – likely exceeded the rate of change and magnitude of any other CE cold phase. The LALIA can therefore be considered as an additional environmental driver of crop failure, famine and plague, as well as a possible trigger for political, societal and economic turmoil (Fig. 4). Outbreak of the Justinian plague between 541 and 543 CE across the Later Roman Empire, as well as its subsequent pandemic development, followed widespread food shortages right after the onset of the LALIA. Spreading apparently from Asia[7], this persisting disease killed several million people and possibly contributed to the reduction of the eastern Roman Empire[1,2]. At the same time, shorter growing seasons and subsequent nutritional deficiencies in people and livestock probably initiated large-scale pastoral movements toward China (Supplementary Information).

While the political situation in Mongolia during the 6th century is not fully understood, it is presumed that conflicts among nomadic groups and regimes in northern China culminated in the replacement of the Rouran as the dominant steppe power by the Türks in 551 CE. This suggests there were major upheavals taking place in central Asia as early as the 550s, which

gradually embroiled much of the central Eurasian steppe region, continuing into the 560s and 580s. The Avars arrived north of the Black Sea ~550 CE (Fig. 4), entered into diplomatic relations but also military conflict with the Romans, and ultimately settled in modern Hungary[11]. Renewed turmoil in central Asia reached the peripheral sedentary empires in the 620s. The Türk ruler, Illig Qaghan raided and invaded north China in the 620s, but after 626 experienced internal wars and Tang counterattacks, leading to the defeat and collapse of the eastern Türk Empire in 630 CE[13]. The western Türks, expanding across central Asia, apparently reached the frontiers of empires east of the Black Sea where, in 625, Emperor Heraclius established diplomatic contacts with "Türks from the East" (Supplementary Information). This alliance prompted the Türks' attacks on Persia through the Caspian Gates that likely played an important role in Heraclius' strategic victory over the Persians.

In a period partly overlapping with the LALIA, the Proto-Slavic dialects spread from a yet unknown homeland across most of continental Europe. Archaeological evidence of Slavic populations in the 6th and 7th centuries suggests they originated in the greater Carpathian region[9], but the motivation for their expansion remains unclear. Westward-moving steppe people like the Avars, as well as opportunities for trading or developing unexploited border regions abandoned by the Roman administration, have been suggested as impetus for the movement of Slavic-speaking people[10]. The Avars' arrival in Pannonia may also have reinforced the political opportunity seized by the departing Lombards who went on to invade Italy in 568 CE[30]. Insofar as cooling affected the Arabian Peninsula (Figs. 1b, S8), the expected precipitation surplus together with reduced evapotranspiration during parts of the LALIA could have boosted scrub vegetation as fodder over arid areas, and thus indirectly contributed to the rise of the Islamic Empire[12]. Larger camel herds may have facilitated transportation of the Arab armies and their supplies during the substantial conquests in the 7th century[12], during which the reconstructed fraction of human land use appears relatively high in the Arabian Peninsula (Fig. S15).

While any hypothesis of a causal nexus between the volcanic-induced 6th century unprecedented thermal shock and subsequent plague outbreaks, rising and falling empires, human migrations, as well as political upheaval requires caution, our newly obtained knowledge of the multidimensional impact of the LALIA fits in well with the major transformative events that occurred in Eurasia during that time. In light of a still inadequate understanding of the various push-pull factors that may have been involved in long-distance population movements, and of the role they have played in human history, our ability to bring into historical analyses what we do know about past climatological and ecological consequences is particular relevant. To overcome reductionist approaches, the use of paleoclimatic evidence in historical arguments has to be combined with multifactor analyses and non-deterministic explanations. Case-by-case assessment will further increase our perception of the environmental conditions under which historical events occurred.

Methods

Tree-ring sampling. All 660 TRW samples were collected from living or dead larch (*Larix sibirica* Ldb.) trees at five high-elevation, near timberline, sites in the Russian Altai-Sayan Mountains. A total of 234,399 individual TRW measurements were performed and the resulting raw time-series were visually and statistically cross-dated to the corresponding calendar years. Examples of the sampling sites are provided in Figure S1, and detailed information on the different TRW subsets as well as the subsequent chronologies is described in Table S2. The temporal behaviour of the new TRW dataset is denoted in Figure S2, including details on common growth variability (Fig. S2a) and sample distribution (Fig. S2b). Eleven annually resolved measurements of the ^{14}C to ^{12}C isotopic ratio between, 770 and 780 CE, were made as an independent, non-dendrochronological dating confirmation[20] of the relict Altai samples (Supplementary Information).

Chronology development. Alignment of the raw TRW measurement series by their innermost ring, ideally representing cambial age at the pith, facilitated the assessment of growth trends and levels. The resulting growth curves, the so-called Regional Curves (RCs) commonly describe trends of negative exponential shape, with very little differences between the five sites and the living and relict material. Splitting the data horizontally[5], into four consecutive intervals of 500 years, reveals similar growth levels after ~500 CE but slightly wider annual increments before (Fig. S2b). An assessment of the mean segment length (MSL) and average growth rate (AGR) of the raw TRW measurement series from the five sampling sites, as well as by sample type (Table S2), reveals an exceptionally high degree of data homogeneity in space and time. The observed similarities in AGR and consistency in the MSL/AGR association among the various data subsets denotes their compatibility also with respect to growth rates and trends. At the same time, the observed relationship between MSL and AGR in the raw TRW series emphasizes the need for tree-ring standardization (detrending) prior to any meaningful interpretation of externally forced variations, i.e. the putative climatic signal within the larch TRW measurements must be separated from the prevailing background noise (Supplementary Information). The combined living and relict TRW chronologies from the five sites in the Altai correlate at 0.93 (p <0.0001) over 1486-1814 CE. Pearson's correlation coefficients between the newly developed TRW chronologies from five sites in the Russian Altai are significantly positive over most of the last centuries (Table S2). Moving 31-year inter-series correlations (*Rbar*) between these records, from 1677 and 1992, range from 0.53-0.87 with a mean of 0.72 (Fig. S4a).

Climate sensitivity. Growth-climate response analyses of the new Altai TRW RCS larch chronology were calculated against monthly resolved temperature means (°C) and precipitation totals (mm/day) extracted from different gridded products (Supplementary Information), averaged over different spatial domains in central Asia, over different time periods during the last 100 years. All correlations with precipitation were non-significant,

whereas a clear relationship between TRW formation and June-August temperatures was found (Supplementary Information). The growth-climate linkage was tested for temporal and spatial stability (Fig. S7, S7). Decadal-scale variability during the 20th century is most obvious in the central European (45-50°N and 10-15°E) JJA temperature mean (Fig. S7a), with below average cooling in the 1910s, a warming peak in the 1940s and a sharp increase from ~1980 onwards. The overall variability and trend in the central Asian (45-50°N and 85-90°E) JJA temperature mean is, however, significantly lower and the rapid warming of the 1980s and 1990s is less distinct (Fig. S7b).

Historical assessment. Because the Chinese and Roman records use different names for them, the details and identifications of some of the central Asian groups in the ancient records are often confusing and controversial. Nevertheless, it is clear that political turbulence in central Asia was underway when the extreme summer cooling began, and peaked when a new political order emerged from the second half of the 6th century, deeply affecting the peripheral areas of Rome, Sasanian Persia and China. The main questions concerning the identifications mentioned in the text are provided in the Supplementary Information.

References

1. *The Years Without Summer: Tracing A.D. 536 and its Aftermath*. (ed Gunn, J. D.) British Archaeological Reports International, Archaeopress (2000).
2. McCormick, M. *et al*. Climate Change during and after the Roman Empire: Reconstructing the Past from Scientific and Historical Evidence. *J. Interdis. Hist.* **43**, 169-220 (2012).
3. Czeglédy, K. From East to West: The Age of Nomadic Migrations in Eurasia. *Archivum Eurasiae Medii Aevi* **3**, 25-126 (1983).
4. Cook, E. R. in *The Ancient Mediterranean Environment between Science and History* (ed Harris W. V.) 89-102 Brill (2013).

5. Büntgen, U. *et al*. 2500 years of European climate variability and human susceptibility. *Science* **331**, 578-582 (2011).

6. Hsiang, S. M., Burke, M. & Miguel, E. Quantifying the influence of climate on human conflict. *Science* **341**, 6151 (2013).

7. Harbeck, M. *et al*. Yersinia pestis DNA from skeletal remains from the 6th century AD reveals insights into Justinianic plague. *PLoS Pathog* **9 (5)**, e1003349 (2013).

8. Demandt, A. *Die Spätantike. Römische Geschichte von Diocletian bis Justinian 284-565 n. Chr.* C.H. Beck (2007).

9. Barford, P. M. Slavs Beyond Justinian's Frontiers. *Studia Slavica et Balcanica Petropolitana* **4**, 21-32 (2008).

10. Heather, P. *Empires and Barbarians. Migration, Development and the Birth of Europe* Pan Macmillan (2009).

11. Golden, P. in *Turko-Mongol Rulers, Cities and City Life* (ed D. Durand-Guédy) 21-74 Brill (2013).

12. Kennedy, H. N. *The Armies of the Caliphs: Military and Society in the Early Islamic State* Routledge (2001).

13. Fei, J., Zhou, J. & Hou, Y. Circa A.D. 626 volcanic eruption, climatic cooling, and the collapse of the Eastern Turkic Empire. *Clim. Change* **81**, 469-475 (2007).

14. Sigl, M. *et al*. Timing and climate forcing of volcanic eruptions for the past 2,500 years. *Nature* **523**, 543-549 (2015).

15. Miller, G. H. *et al*. Abrupt onset of the Litte Ice Age triggered by volcanism and sustained by sea-ice/ocean feedbacks. *Geophys. Res. Lett.* **39**, L02708 (2012).

16. McGregor, H. V. *et al*. Robust global ocean cooling trend for the pre-industrial Common Era. *Nature Geosci.*. **8**, 671-677 (2015).

17. Steinhilber, F., Beer, J. & Fröhlich, C. Total solar irradiance during the Holocene. *Geophys. Res. Lett.* **36**, L19704 (2009).

284 18. PAGES 2k Consortium. Continental-scale temperature variability during the past two millennia.
285 *Nature Geosci.* **6**, 339-346 (2013).
286 19. Braconnot, P. *et al*. Evaluation of climate models using palaeoclimatic data. *Nature Clim.*
287 *Change* **2**, 417-424 (2012).
288 20. Myglan, V. S., Oidupaa, O. C. & Vaganov, E. A. A 2367-year tree-ring chronology for
289 the Altay-Sayan region (Mongun-Taiga Mountain Massif). *Archaeol. Ethnol. Anthropol.*
290 *Eurasia* **40**, 76-83 (2012).
291 21. Agatova, A. R. *et al*. Glacier dynamics, palaeohydrological changes and seismicity in
292 southeastern Altai (Russia) and their influence on human occupation during the last 3000
293 years. *Quat. Int.* **324**, 6-19 (2014).
294 22. Kausrud, K. L. *et al*. Modeling the epidemiological history of plague in Central Asia:
295 Palaeoclimatic forcing on a disease system over the past millennium. *BMC Biol*. **8**,
296 112 (2010).
297 23. Schmid, B. V. *et al.* Climate-driven introduction of the Black Death and successive plague
298 reintroductions into Europe. *Proc. Natl. Acad. Sci. U.S.A* **112**, 3020-3025 (2015).
299 24. Büntgen, U. *et al*. Extra-terrestrial confirmation of tree-ring dating. *Nature Clim. Change*
300 **4**, 404-405 (2014).
301 25. Esper, J., Büntgen, U., Frank, D. C., Nievergelt, D. & Liebhold, A. 1200 years of regular
302 outbreaks in alpine insects. *Proc. R. Soc. B* 274, 671-679 (2007).
303 26. Saeed, S., Van Lipzig, N., Müller, W. A., Saeed, F. & Zanchettin, D. Influence of the
304 circumglobal wave-train on European summer precipitation. *Clim. Dyn.* 43, 503-515
305 (2014).
306 27. Jungclaus, J. H., Lohmann, K. & Zanchettin D. Enhanced 20th-century heat transfer to the
307 Arctic simulated in the context of climate variations over the last millennium. *Clim. Past*
308 **10**, 2201-2213 (2014).

28. Barriopedro, D., Fischer, E. M., Luterbacher, J., Trigo, R. M. & Garcia-Herrera, R. The hot summer of 2010: Redrawing the temperature record map of Europe. *Science* **332**, 220-224 (2011).

29. Esper, J. *et al*. Orbital forcing of tree-ring data. *Nature Clim. Change* **2**, 862-866 (2012).

30. Pohl, W. *Die Awaren: ein Steppenvolk in Mitteleuropa 567-822 n. Chr.* C.H. Beck (1988).

Additional information

Supplementary Information (Text, Figures S1-S15, Tables S1-S5, and References 31-184) is linked to the online version of the paper at www.nature.com/nature. Information on reprints and permissions is available at www.nature.com/reprints. Readers are welcome to comment on the online version of the paper. Correspondence and requests should be addressed to U.B. (buentgen@wsl.ch), and to M.M (sohp@fas.harvard.edu) concerning the historical component of this work.

Acknowledgments

B. Bramanti, B.M.S. Campbell, S.M. Hsiang, C. Oppenheimer, as well as three anonymous referees kindly commented on earlier versions of this article. D. Galvan helped with the radiocarbon measurements (within the WSL-internal COSMIC project), L. Hellmann provided technical support for Figure 4 (via E. Mayr-Stihl Foundation), and D. Zanchettin contributed insight on positive feedback loops. U.B. was supported by the Czech project 'Building up a multidisciplinary scientific team focused on drought' (No. CZ.1.07/2.3.00/20.0248). Support for PAGES activities is provided by the US and Swiss National Science Foundations, US National Oceanographic and Atmospheric Administration and by the International Geosphere-Biosphere Programme. All tree-ring data from the Altai were collected and measured through support from the Russian Science Foundation (project 14-14-00295). Historical evidence was extracted from work ongoing at SoHP, Harvard

University. Data used in this study will be archived with associated metadata at http://www.ncdc.noaa.gov for routine public access.

Author contributions

U.B. designed the study, together with M.M., and U.B. performed most of the analyses with support from all authors. V.S.M. and A.V.K. conducted fieldwork in the Russian Altai and developed the corresponding tree-ring chronologies. M.M., N.D.C., J.O.K., M.A.C.V. and F.C.L. added historical insight. J.J. and S.W. provided model output, and L.W. measured and analysed ^{14}C. F.C.L. compiled multi-proxy LALIA evidence for the Northern Hemisphere. U.B. wrote the paper together with F.C.L., M.M., N.D.C., P.J.K., J.E., J.L. and W.T. All authors edited the various manuscript versions and contributed to long-lasting discussions.

Competing financial interests

The authors declare no competing financial interests.

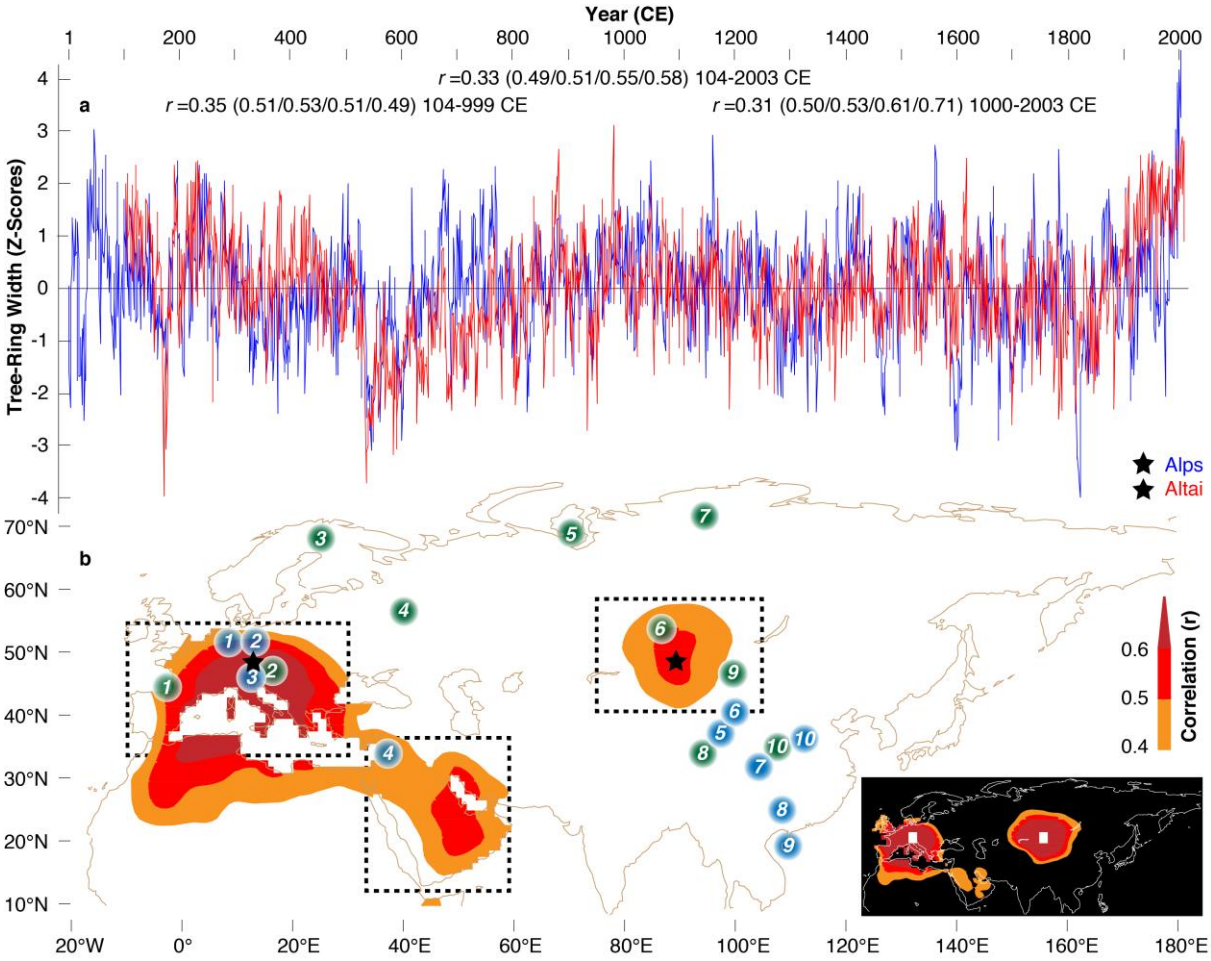

Figure 1 | Growth coherency and climate sensitivity. a, Normalized Alpine (*3*) and Altai RCS TRW chronologies, with correlation coefficients referring to the original and smoothed (20/40/80/120yr) records as well as full and split (</>1000 CE) periods. **b**, Corresponding spatial correlations (1900-2003) against gridded JJA temperatures. Locations of ten temperature and hydroclimatic proxies (green and blue) (Table S5), with frames indicating the regions for which anthropogenic land-use changes were modelled (Fig. S15). Inset reveals spatial correlations of gridded JJA temperatures from the Alpine (45-50°N and 10-15°E) and Altai (45-50°N and 85-90°E) against the same gridded dataset over Eurasia (Fig. S8).

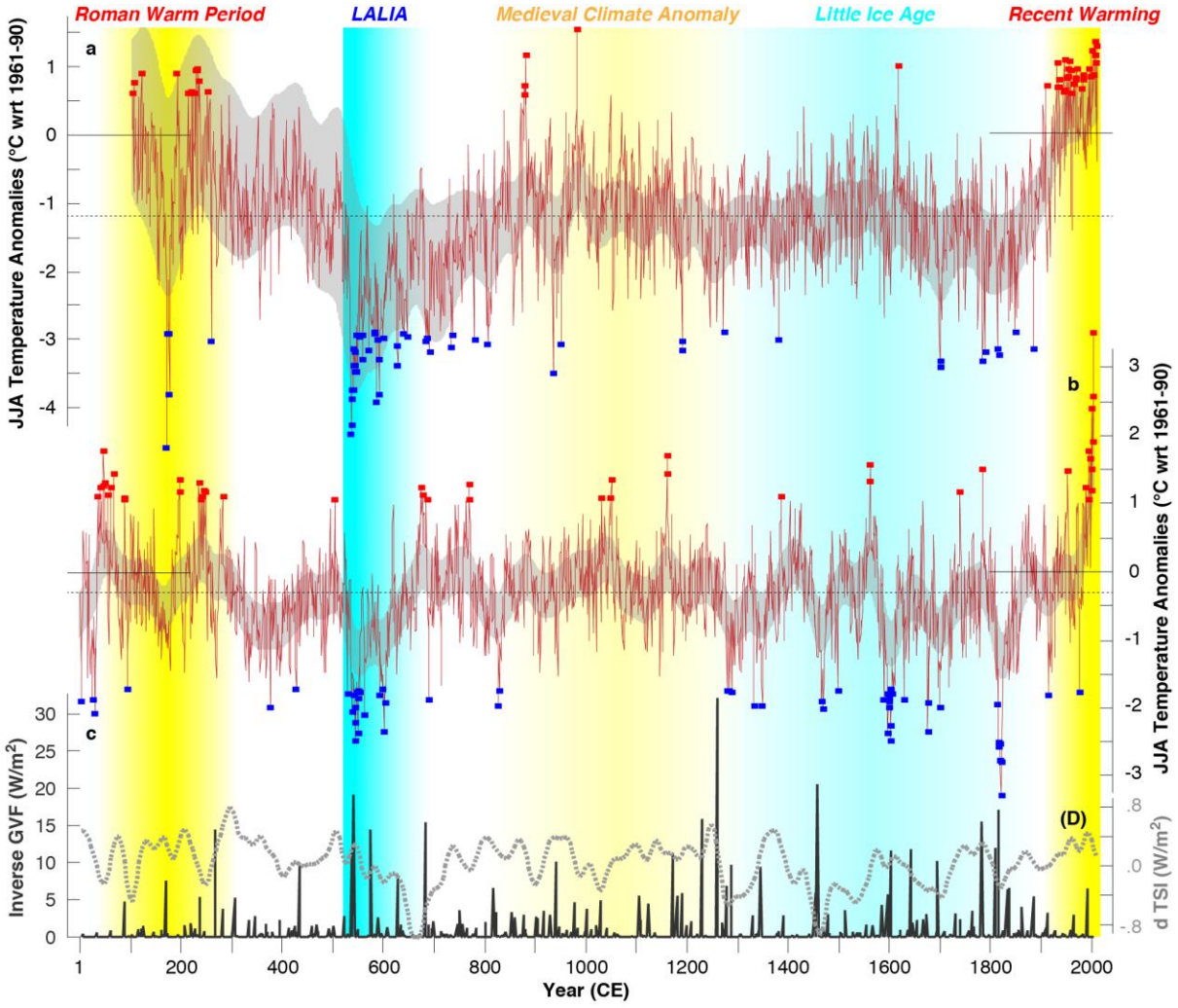

Figure 2 | Eurasian summer temperatures during the Common Era. a-b, Reconstructed temperatures from the Russian Altai and the European Alps[5], with blue and red boxes indicating (51/47) positive and (53/57) negative annual extremes (>2 standard deviations), respectively. Grey background shadings refer to reconstruction uncertainty after 80-year low-pass filtering (Fig. S9). **c**, Ice-core derived global estimates of volcanic (dark grey)[14] and **d**, solar (light dashed grey)[17] forcing.

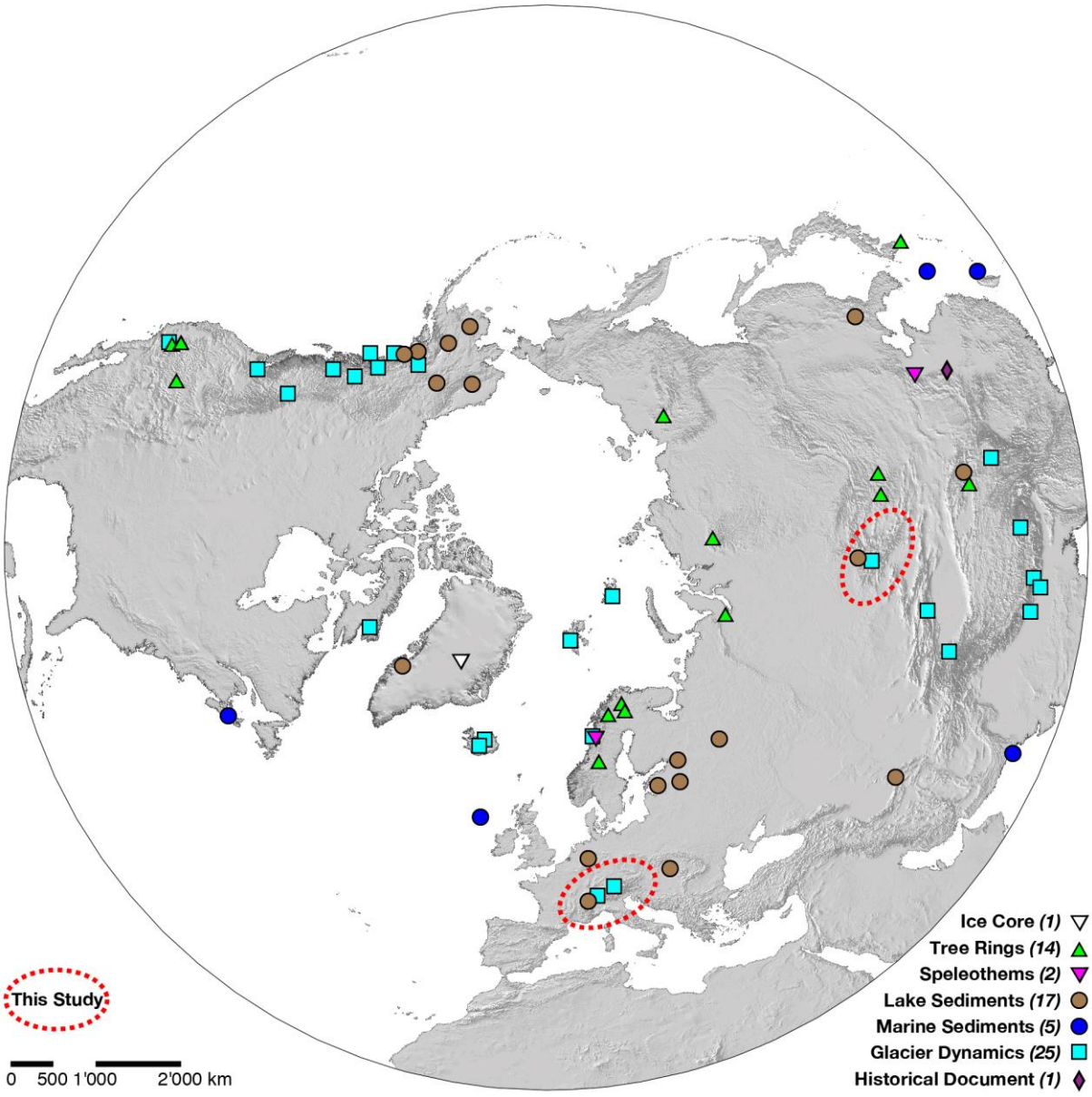

Figure 3 | Multi-proxy evidence of the LALIA. Compilation of 65 temperature-sensitive records from seven different proxy archives distributed over the extra-tropical Northern Hemisphere (>20°N). All proxy records contain below average values between 536 and ~660 CE, or mention of their displaying a distinct cooling during this interval has been published (Table S3).

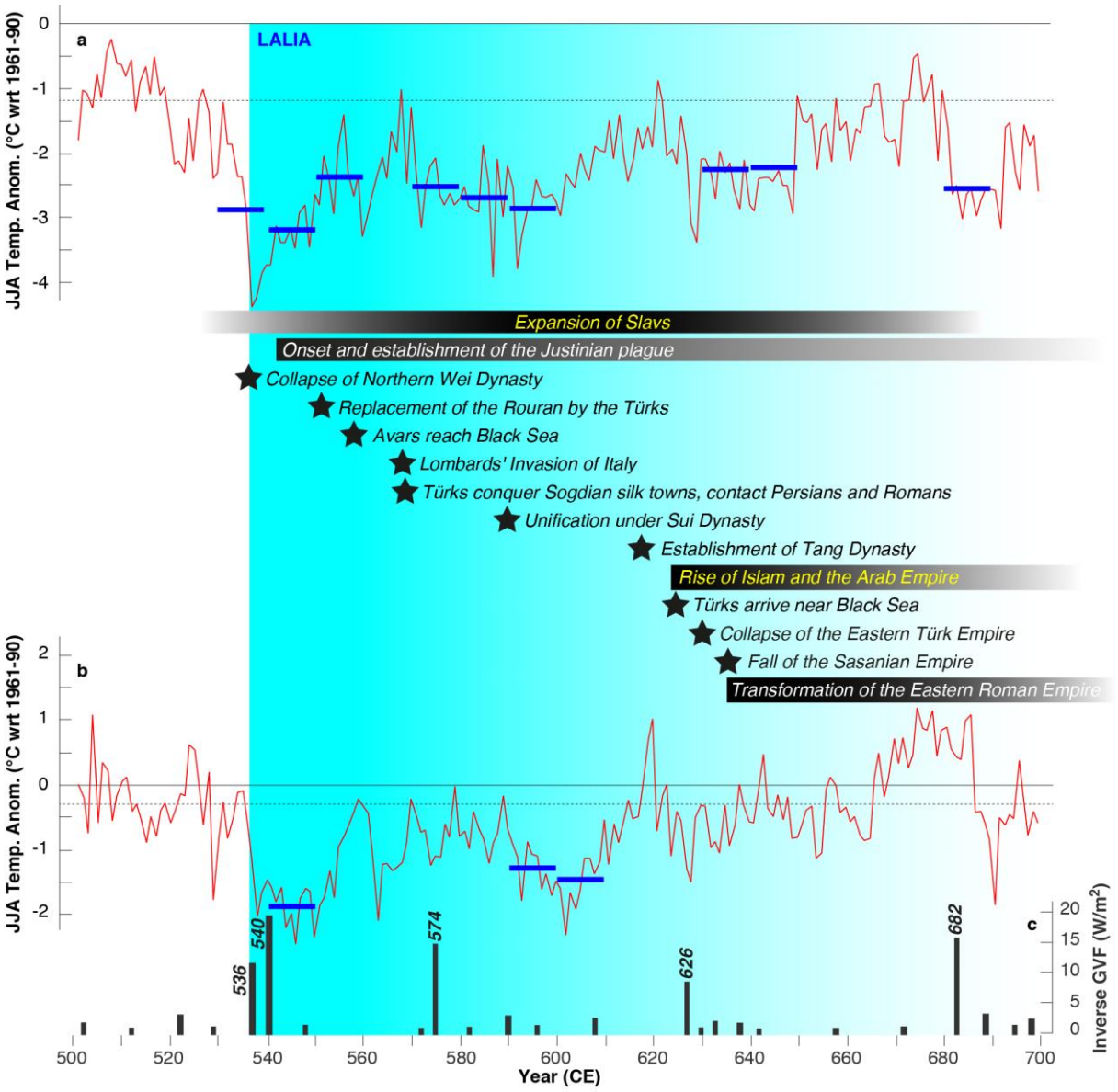

Figure 4 | Climate variability and human history during the LALIA. a-b, Reconstructed summer temperatures from the Russian Altai and the European Alps, together with **c**, estimated volcanic forcing[14]. Blue lines highlight the coldest decades of the LALIA that range among the ten coldest decades of the CE. Horizontal bars, shadings and stars refer to major plague outbreaks, rising and falling empires, large-scale human migrations, as well as political turmoil (Supplementary Information).